Geophysical Research Letters

Supporting Information for

Mass Balance Reassessment of Glaciers Draining into the Abbot and Getz Ice Shelves of West Antarctica

S.J. Chuter[1], A. Martín-Español[1], B. Wouters[2], J.L. Bamber[1]

[1]Bristol Glaciology Centre, School of Geographical Sciences, University of Bristol, Bristol, UK, BS8 1SS

[2] Institute for Marine and Atmospheric Research Utrecht, Utrecht University, Utrecht, Netherlands

Contents of this file

Introduction

This supplementary material provides supporting figures and tables to the main text in addition to supplementary methods outlining the calculation of ice shelf thickness. Figures S1 and S2 show the changes in ice shelf thickness since 1994, which was used to provide temporal adjustments to the CryoSat-2 thickness measurements. Figures S3 and S4 show the SMB anomaly trends from 2006 to the present day, illustrating the effect of climate driven processes on changes in mass imbalance. Figures S5 and S6 show RATES results for both basins in the Bellingshausen Sea and Amundsen Sea Sectors for 2003-2013. Figure S7 shows a comparison of Operation Ice Bridge Data with the CryoSat-2 ice shelf thickness product over the Getz Ice Shelf. The tables included in this supplement show the validation statistics for the CryoSat-2 ice thickness product (Tables S1 and S2) and the studies references in the comparison boxes (Tables S3 and S4). Table S5 is results for the RATES project using the same basin extents as our mass budget assessment.

Supplementary Methods

Ice Shelf thickness calculation

Ice shelf thickness is calculated using two years (2013-2014) of CryoSat-2 Baseline B Level L2i radar altimetry measurements and the assumption of hydrostatic equilibrium:

$$H_i = \frac{(e - \delta)\rho_w}{\rho_w - \rho_i}$$

Where (H_i) is the ice equivalent thickness (the thickness of the ice if the whole column was at the meteoric ice density), δ is the air content of the firn layer expressed as meters of ice equivalent, *e* is the freeboard (elevation of the ice shelf with respect to sea level), ρ_w and ρ_i are the densities of water (1027kg m^3) and ice respectively (917 kg m^3).

Ice shelf freeboard is determined from the ellipsoid elevation measurements using the EIGEN-6C4 Geoid [*Förste et al.*, 2014] and DTU12MDT [*Knudsen and Andersen*, 2012] mean dynamic topography (MDT) datasets. MDT is not directly observable over the ice shelves, therefore the mean MDT value at the ice shelf front was extrapolated as the value for the whole ice shelf. The mean MDT value for the Abbot and Getz ice shelves are -0.99 m and -0.81 m respectively.

Corrections for firn air depth content is provided from output of a time-dependent Firn Densification Model (FDM) including surface melt processes [*Ligtenberg et al.*, 2014], which is forced by the RACMO2.3 regional climate model. The model is run at 27 km spatial resolution, the outputs of which are resampled to 1 km to match the resolution of the ice thickness product. Firn air content has large spatial variability over short spatial length scales, particularly at the grounding line [*van den Broeke et al.*, 2008; *Griggs and Bamber*, 2011] with a mean modelled value of 21.01 m and 23.86 m at the Abbot and Getz grounding lines, respectively.

Ice Shelf Thickness Uncertainty

An estimate of ice thickness uncertainty can be ascertained by error propagation of the components of the Hydrostatic Equilibrium equation. Ocean water density varies spatially dependent on salinity and temperature, with 1024 kg m^3 [*Bamber and Bentley*, 1994] to 1029 kg m^3 [*Fricker et al.*, 2001] being used in previous studies. Therefore an uncertainty of ± 5 kg m^3 is used in our calculations, the same as the uncertainty estimate in the previous ERS-1 data product [*Griggs and Bamber*, 2011].

The density of ice can vary between 912 kg m^3 and 922 kg m^3 (based on observations over the Amery Ice Shelf) [*Fricker et al.*, 2001], therefore we use ± 5 kg m^3 as uncertainty estimates for ice density. Again this is the same uncertainty that was used in the previous data product [*Griggs and Bamber*, 2011].

Uncertainty in the FDM is estimated to be 10% [*Depoorter et al.*, 2013a]. Uncertainty in ice shelf freeboard is quantified as the standard deviation between $\Delta h/\Delta t$ corrected ICESat laser altimetry and the CS2 Ice Shelf DEM on an individual shelf basis.

This results in a mean ice thickness uncertainty of ±55 m and ±40 m for the Getz and Abbot ice shelves respectively (the values typically vary between 40 and 60 m around the continent). This compares with a spatially invariant error of ±150 m for the ice shelf sectors in Bedmap2 and uncertainties of 10-80 m in other IOM assessments [*Rignot et al.*, 2008; *Shepherd et al.*, 2012].

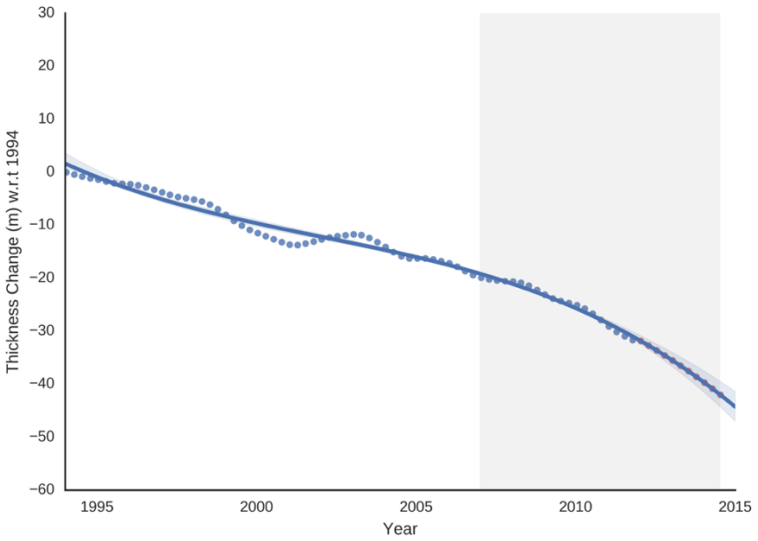

Figure S1 - Getz ice shelf mean $\Delta T/\Delta t$ from 1994 to 2015. The 3-monthly thickness change values w.r.t 1994 are shown as the blue points. A 3rd order polynomial trend line is fitted, with the light blue shaded region representing the 95% confidence interval. As observations were only available up to the end of 2011 the polynomial regression model was used to extend the record to 2015, the same time stamp as the CryoSat-2 ice thickness and Landsat-8 velocity data sets. The grey region shows the timespan between the velocity data sets.

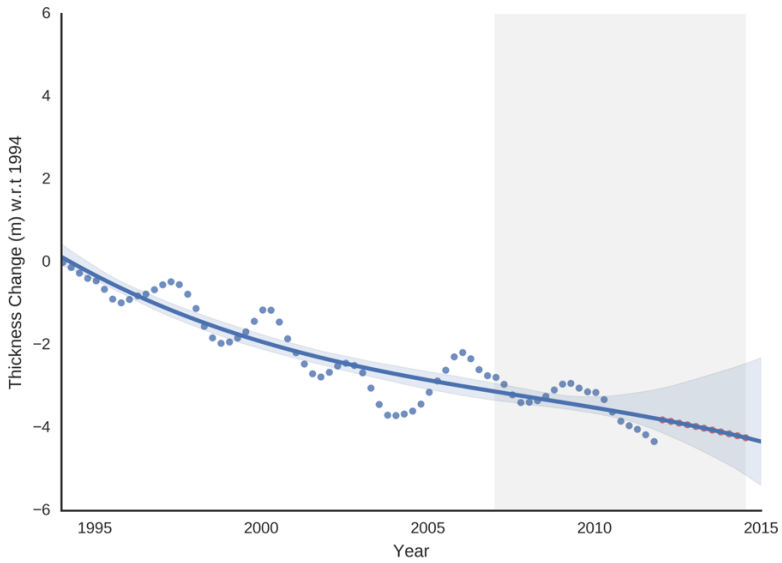

Figure S2 - Abbot ice shelf mean $\Delta T/\Delta t$ from 1994 to 2015. The 3-monthly thickness change values w.r.t 1994 are shown as the blue points. A 3rd order polynomial trend line is shown, with the light blue region representing the 95% confidence of the regression. As observations were only available up to the end of 2011 the polynomial regression model was used to extend the record to 2015, the same time stamp as the CryoSat-2 ice thickness and Landsat-8 velocity data sets. The grey region shows the time span between the two velocity data sets.

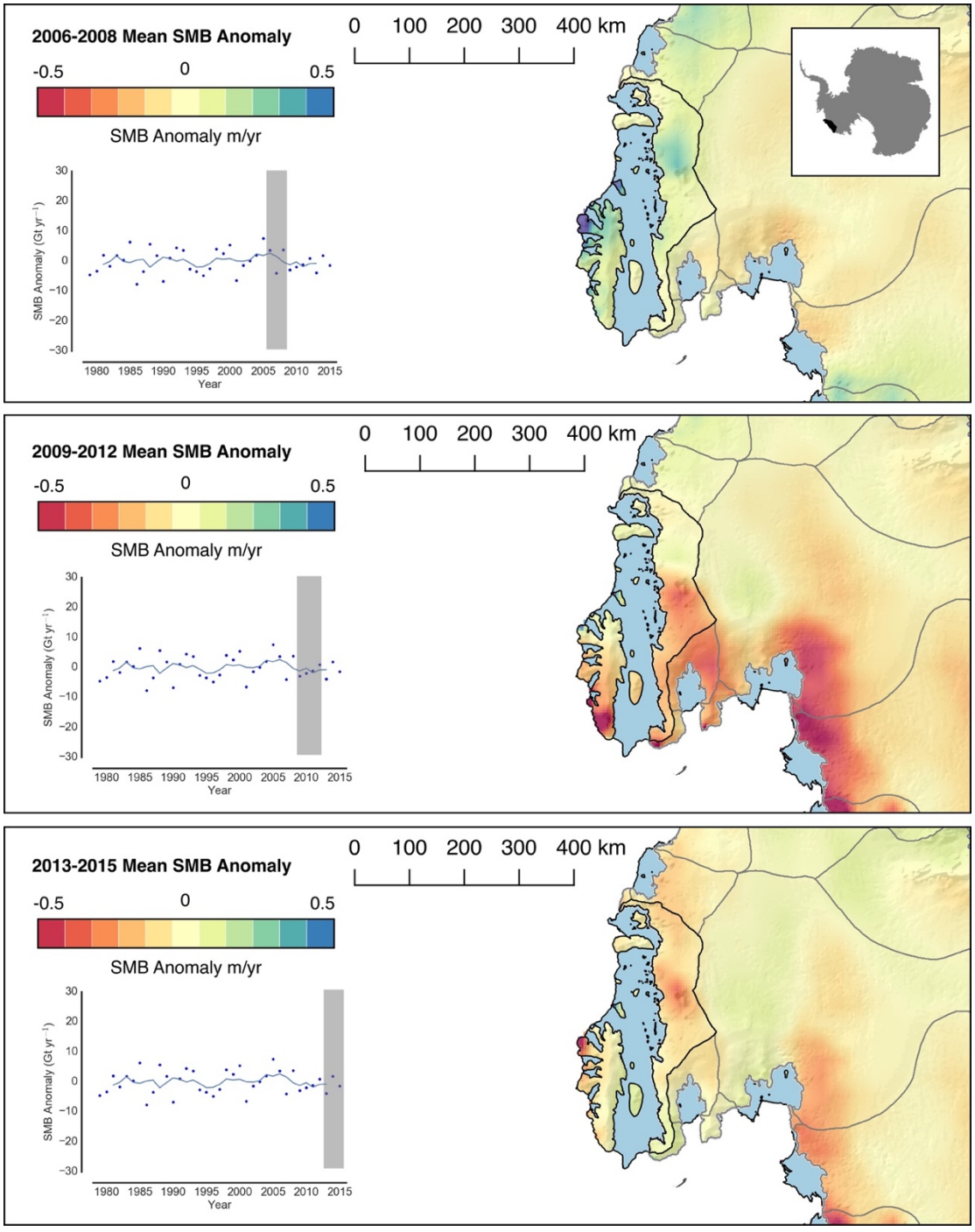

Figure S3 – Abbot RACMO2.3 SMB Anomalies with respect to a 26-year baseline period between 1979-2005. The basin draining into the Abbot Ice Shelf is shown in black, with other basins shown in grey [*Depoorter et al.*, 2013b]. Inset plots show the annual SMB anomalies from 1979 to the present day, with a 5-year running mean trend. Grey shaded regions on the plots represent the corresponding time period shown in the map.

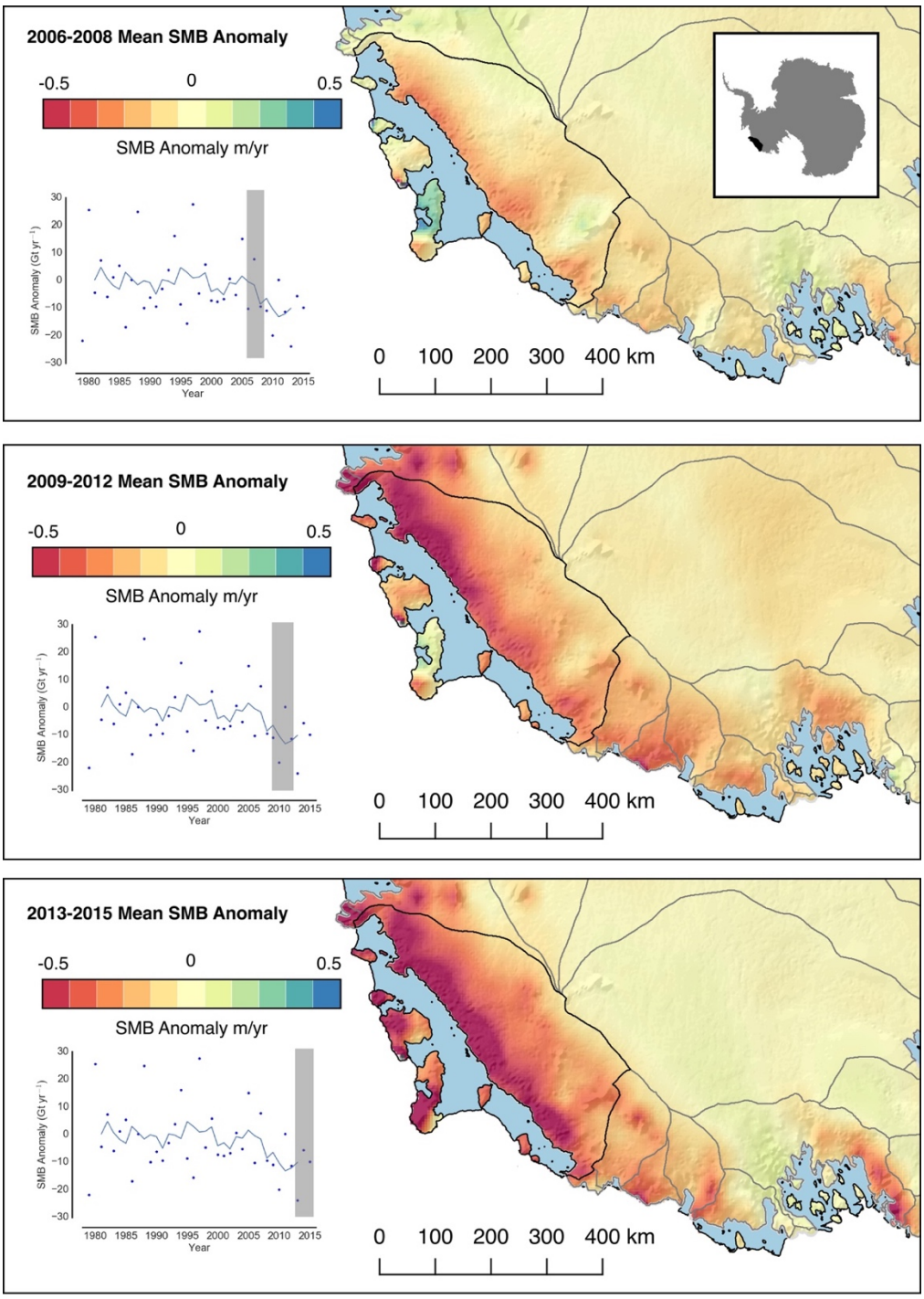

Figure S4– Getz RACMO2.3 SMB Anomalies with respect to a 26-year baseline period between 1979-2005. The Getz drainage basin is shown in black, with others shown in grey [*Depoorter et al.*, 2013b]. Inset plots show the annual SMB anomalies from 1979 to the present day, with a 5-year running mean trend. Grey shaded regions on the plots represent the corresponding temporal period of the map.

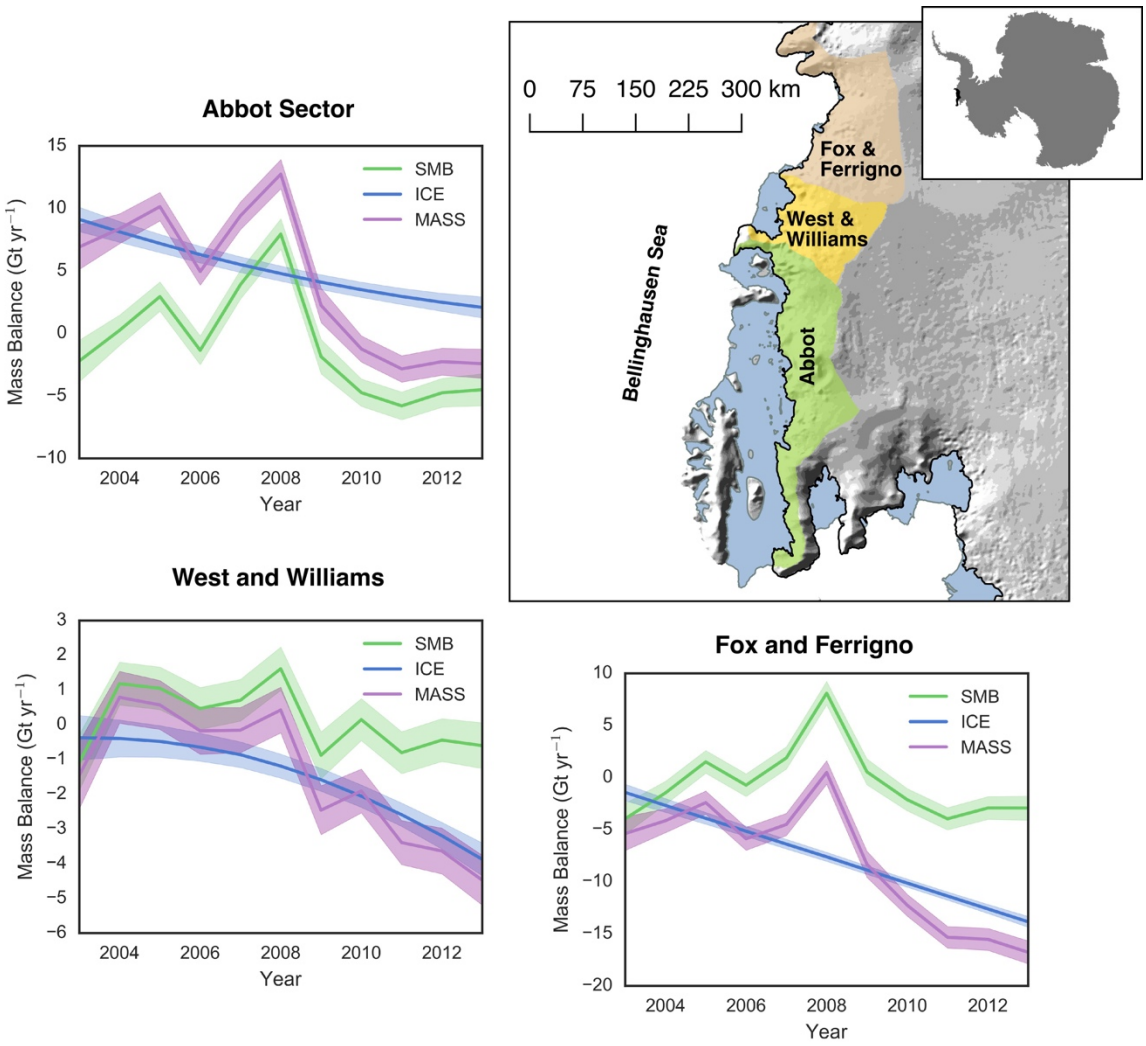

Figure S5 – Results from RATES for the Bellingshausen Sea Sector between 2003-2013, using the same data sets and methodology as Martín-Español *et al*. [2016]. The inset map shows the basin extents used in this study, with the RATES results for each basin shown in the surrounding line plots. The line plots show the overall mass trend (purple), mass changes attributed to surface mass balance (green) and ice dynamics (blue). The lightly shaded regions in each line plot show the 1 σ uncertainty for each modelled component. The annual mass balance figures from the RATES project are presented in table S5.

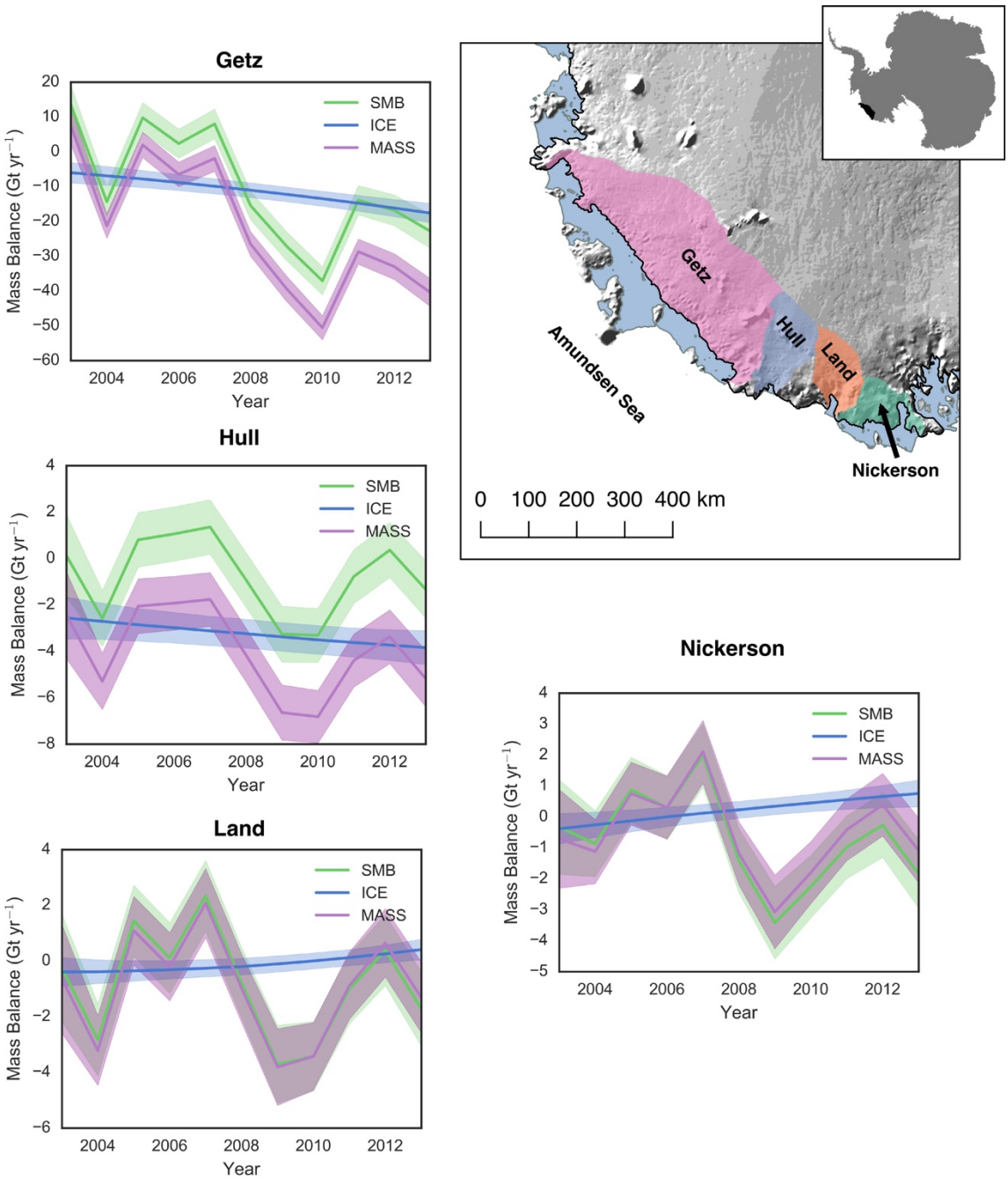

Figure S6 -– Results from RATES for the Getz region between 2003-2013, using the same data sets and methodology as Martín-Español *et al*. [2016]. The inset map shows the basin extents used in this study, with the RATES results for each basin shown in the surrounding line plots. The line plots show the overall mass trend (purple), mass changes attributed to surface mass balance (green) and ice dynamics (blue). The lightly shaded regions in each line plot show the 1 σ uncertainty for each modelled component. The annual mass balance figures from the RATES project are presented in table S5.

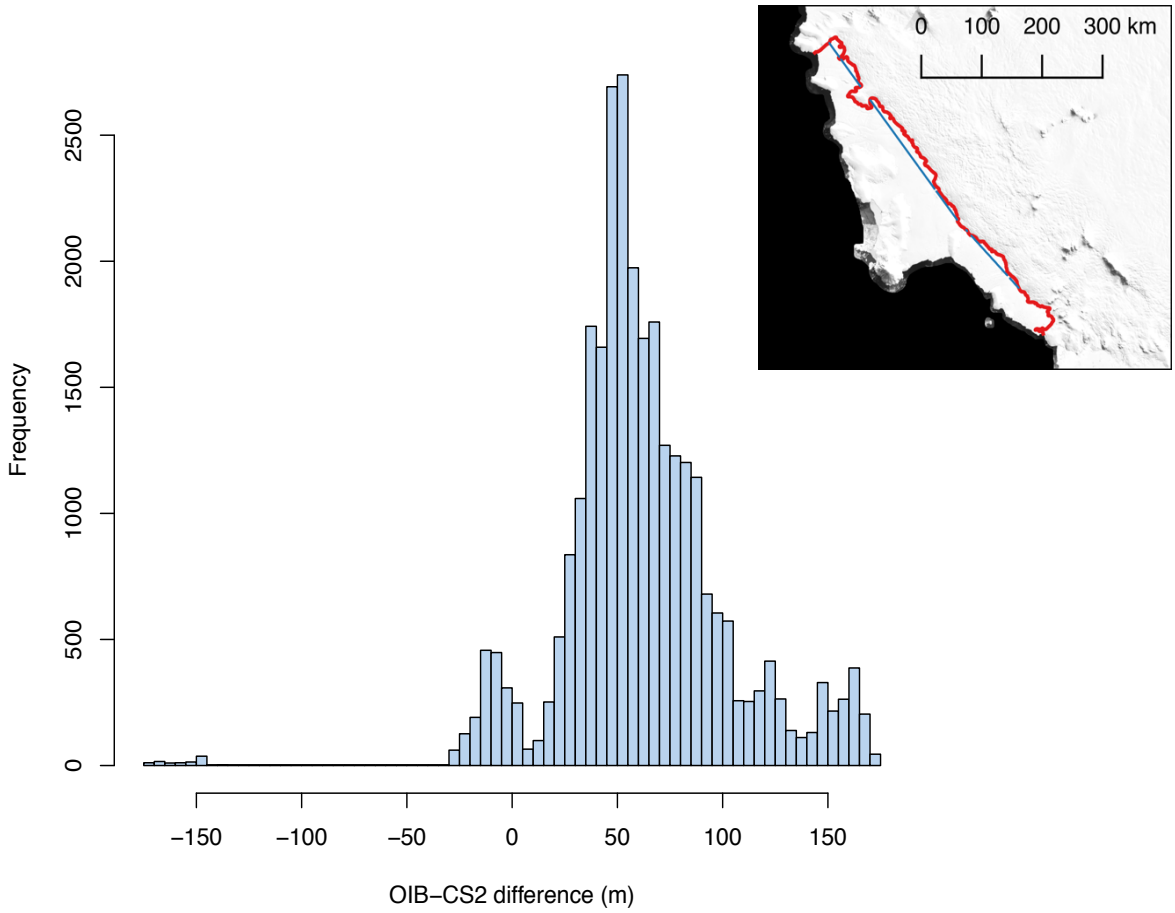

Figure S7 – Histogram plot of differences between the CS2 ice shelf thickness product (time stamp of 2013-2014) and thickness data from an Operation Ice Bridge (OIB) flight line acquired on 11/11/2014. A 1 km window boxcar filter was applied to the OIB observations to provide better consistency in spatial resolution with the gridded CS2 product. OIB MCoRDS L2 Ice thickness data has depth resolution of ~18 m [Leuschen *et al*, 2016]. Positive differences indicate the CS2 ice thickness product is thinner than OIB. The inset plot shows the location of the flight line (blue) and the grounding line (red) [Depoorter *et al*, 2013b].

Table S1. Spatial coverage of CryoSat-2 observations over the Getz and Abbot ice shelves using data from 2013 and 2014. Also included are comparisons with the continental CryoSat-2 data set [*Chuter and Bamber*, 2015] and the ERS-1 data set that formed the ice shelf component of Bedmap2 [*Griggs and Bamber*, 2011].

Ice Shelf	**No Observations**	**% 1 km grid cells filled 2013-2014**	**% Cells filled *Chuter and Bamber* [2015]**	**% Cells filled *Griggs and Bamber* [2011]**
Abbot	147719	73.47	85.96	52.1
Getz	191585	79.87	92.25	53.2

Table S2. Comparison of the Ice Shelf DEM with NASA ICESat laser altimetry within 10 km of the grounding line (ICESat-CryoSat-2). The CryoSat-2 product offers reduced biases and uncertainties compared to previous continental ice shelf thickness data set [*Griggs and Bamber*, 2011].

	This Study		*Chuter and Bamber* [2015]		*Griggs and Bamber* [2011]	
Ice Shelf	$\Delta h/\Delta t$ corrected mean	$\Delta h/\Delta t$ corrected σ	$\Delta h/\Delta t$ corrected mean	$\Delta h/\Delta t$ corrected σ	$\Delta h/\Delta t$ corrected mean	$\Delta h/\Delta t$ corrected σ
Abbot	1.76	3.96	1.48	3.52	-4.66	12.07
Getz	2.96	3.86	2.89	3.54	-8.9	17.32

Table S3. Bellingshausen Sea mass balance studies used for comparison in Figure 3. The Re-assessed result presented in this study is listed in bold.

Study	Method	Time period	Mass Balance (Gt yr^{-1})
Sasgen et al [2013]	Gravimetry	2003-2012	-15±9
Martín-Español et al [2016]	RATES	2003-2006 2007-2009 2010-2013	8.6±3.6 3.4±2.6 -18.6±3.6
McMillan et al [2014]	Radar Altimetry	2010-2013	-12±9
Wouters et al [2015]	Radar Altimetry	2003-2005 2007-2009 2010-2014	5.4±9.8 -0.4±8.7 -7.2±4.7
Rignot et al [2008]	IOM	1992-1995*	-14±9
Sasgen et al [2010]	Gravimetry	2002-2008	-9.2±1.3
Groh and Horwath [2016]	Gravimetry	2002-2016	-9.6±4.9
King et al [2012]	Gravimetry	2002-2010	-7±3
Zwally et al. [2015]	Radar Altimetry	2003-2008	11±3
This Study	**IOM**	**2006-2008**	**8 ± 6**

*Long term 1980-2004 SMB average from RACMO used. Time period listed corresponds to the velocity data used in the study.

Table S4. Getz mass balance studies used for comparison in Figure 3. The Re-assessed result presented in this study is listed in bold.

Study	Method	Time period	Mass Balance (Gt yr^{-1})
Sasgen et al [2013]	Gravimetry	2003-2012	-42±9
Martín-Español et al [2016]	RATES	2003-2006 2007-2009 2010-2013	-11.7±4.9 -31.6±4.4 -48.6±4.6
McMillan et al [2014]	Radar Altimetry	2010-2013	-23±9
Wouters et al [Unpublished]	Radar Altimetry	2010-2013	-18.9±4
Rignot et al [2008]	IOM	1995-1996*	-11±18
Sasgen et al [2010]	Gravimetry	2002-2008	-1.1±1.3
Groh and Horwath [2016]	Gravimetry	2002-2016	-36.2±5.6
Bouman et al [2014]	Gravimetry	2009-2012	-55±9
King et al. [2012]	Gravimetry	2002-2010	-23±3
Zwally et al. [2015]	Radar Altimetry	2003-2008	-16±1
This Study	**IOM**	**2006-2008**	**5 ±17**

*Long term 1980-2004 SMB average from RACMO used. Time period listed corresponds to the velocity data used in the study.

Table S5 – Annual RATES results for drainage sectors in the Amundsen Sea and Bellingshausen Sea Sectors (See figures S5 & S6 for drainage basin locations). The 2006-2008 mean (the epoch of the mass budget reassessment in this study) and 2003-2013 mean is also shown. Drainage sectors from Depoorter *et al* [2013a].

Drainage Basin Sector	2003	2004	2005	2006	2007	2008	2009	2010	2011	2012	2013	2006-2008 Mean	2003-2013 Mean
Abbot	6.91 ± 1.79	8.37 ± 1.19	10.14 ± 1.14	4.95 ± 1.09	9.42 ± 1.11	12.74 ± 1.17	2.24 ± 1.38	-1.24 ± 1.04	-2.84 ± 1.05	-2.26 ± 1.08	-2.42 ± 1.16	**9.04 ± 1.12**	**4.18 ± 1.20**
Wesnet & Williams	-1.45 ± 0.96	0.79 ± 0.75	0.57 ± 0.70	-0.18 ± 0.67	-0.15 ± 0.65	0.42 ± 0.66	-2.46 ± 0.70	-1.91 ± 0.63	-3.39 ± 0.63	-3.63 ± 0.66	-4.47 ± 0.72	**0.03 ± 0.66**	**-1.44 ± 0.70**
Ferrigno & Fox	-5.38 ± 1.62	-4.14 ± 1.15	-2.40 ± 1.11	-5.87 ± 1.10	-4.50 ± 1.07	0.49 ± 1.13	-8.33 ± 1.26	-12.25 ± 1.04	-15.33 ± 1.04	-15.52 ± 1.05	-16.77 ± 1.10	**-3.29 ± 1.10**	**-8.18 ± 1.15**
Nickerson	-0.71 ± 1.60	-1.12 ± 1.04	0.76 ± 1.02	0.31 ± 1.02	2.11 ± 1.02	-1.18 ± 1.02	-3.07 ± 1.19	-1.80 ± 1.00	-0.41 ± 1.00	0.40 ± 1.01	-1.08 ± 1.04	**0.41 ± 1.02**	**-0.53 ± 1.09**
Land	-0.64 ± 1.95	-3.21 ± 1.25	1.09 ± 1.24	-0.21 ± 1.23	2.08 ± 1.24	-0.98 ± 1.23	-3.81 ± 1.38	-3.42 ± 1.21	-0.88 ± 1.21	0.65 ± 1.23	-1.30 ± 1.27	**0.30 ± 1.23**	**-0.97 ± 1.31**
Hull	-2.43 ± 1.88	-5.29 ± 1.22	-2.05 ± 1.18	-1.93 ± 1.16	-1.77 ± 1.16	-4.16 ± 1.16	-6.64 ± 1.19	-6.82 ± 1.13	-4.40 ± 1.14	-3.37 ± 1.16	-5.17 ± 1.21	**-2.62 ± 1.16**	**-4.00 ± 1.24**
Getz	7.45 ± 5.29	-21.28 ± 3.55	1.95 ± 3.66	-6.50 ± 3.53	-1.93 ± 3.72	-26.50 ± 3.54	-39.32 ± 3.65	-50.55 ± 3.46	-28.70 ± 3.62	-32.98 ± 3.70	-40.42 ± 4.01	**-11.64 ± 3.60**	**-21.71 ± 3.79**